Available online at www.sciencedirect.com

ScienceDirect

Ceramics International 39 (2013) 8693–8700

CERAMICS INTERNATIONAL

www.elsevier.com/locate/ceramint

Structural, optical and photocatalytic properties of hafnium doped zinc oxide nanophotocatalyst

M. Ahmad[a,b,*], E. Ahmed[a], Z.L. Hong[b], Z. Iqbal[a], N.R. Khalid[a,b], T. Abbas[c], Imran Ahmad[a], A.M. Elhissi[d], W. Ahmed[d]

[a]*Department of Physics, Bahauddin Zakariya University, Multan 60800, Pakistan*
[b]*State Key Laboratory of Silicon Materials, Department of Materials Science & Engineering, Zhejiang University, Hangzhou 310027, China*
[c]*Institute of Industrial Control System, Rawalpindi, Pakistan*
[d]*Institute of Nanotechnology and Bioengineering, University of Lancashire, Preston PR1 2HE, United Kingdom*

Received 5 February 2013; received in revised form 13 April 2013; accepted 15 April 2013
Available online 21 April 2013

Abstract

A series of novel hafnium (Hf) doped ZnO nanophotocatalyst were synthesized using a simple sol–gel method with a doping content of up to 6 mol%. The structure, morphology and optical characteristics of the photocatalysts were characterized by XRD, SEM, TEM, FTIR, XPS, DRS and PL spectroscopy. The successful synthesis and chemical composition of pure and doped ZnO photocatalysts were confirmed by XRD and XPS. DRS confirmed that the spectral responses of the photocatalysts were shifted towards the visible light region and showed a reduction in band gap energy from 3.26 to 3.17 eV. Fluorescence emission spectra indicated that doped ZnO samples possess better charge separation capability than pure ZnO. The photocatalytic activity of Hf-doped ZnO was evaluated by the methylene blue (MB) degradation in aqueous solution under sunlight irradiation. Parameters such as irradiation time and doping content were found effective on the photoactivity of pure ZnO and Hf-doped ZnO. The photocatalysis experiments demonstrated that 2 mol% Hf-ZnO exhibited higher photocatalytic activity as compared to ZnO, ZnO commercial and other hafnium doped ZnO photocatalysts and also revealed that MB was effectively degraded by more than 85% within 120 min. The enhanced photoactivity might be attributed to effective charge separation and enhanced visible light absorption. It was concluded that the presence of hafnium within ZnO lattice could enhance the photocatalytic oxidation over pure ZnO.

Keywords: A. Sol–gel; D. ZnO; Hf-doped ZnO; Methylene blue; Photocatalysts

1. Introduction

ZnO, a wide band compound semiconductor material is currently the subject of vigorous development and study programs because of its potential applications in many areas such as environmental pollution control, field emission displays, photocatalysis, solar cell windows, gas sensors and pharmaceuticals [1–4]. ZnO is a biocompatible antibacterial compound that exhibits high mechanical, thermal and chemical stability. Owing to its remarkable physical and chemical qualities, it can be used extensively in information technology, biotechnology and environmental technology [5,6]. ZnO has also been considered as a suitable alternate for TiO_2 photocatalyst owing to its similar band gap, absence of toxicity, high chemical stability and lower cost. Moreover, it exhibits better performance in the degradation of organic dye molecules in both acidic and basic media. The intrinsic defects of ZnO are advantageous to setting up catalytic systems, which are expected to degrade the environmental pollutants [4]. The main advantage of ZnO as compared with TiO_2 is that it can absorb larger fraction of the UV spectrum than TiO_2 [7,8]. The common scheme for the photocatalytic destruction of organic pollutants encompasses the following three steps: (1) when the energy ($h\nu$) of a photon is equal to or higher than the band gap (E_g) of the semiconductor, an electron is excited to conduction band (CB), with simultaneous generation of a hole in the valance band (VB); (2) then the photoexcited electrons and

*Corresponding author at: Department of Physics, Bahauddin Zakariya University, Multan 60800, Pakistan. Tel.: +92 61 9210091; fax: +92 61 9210098.
E-mail addresses: mzkhm73@gmail.com, mzkhm@yahoo.com (M. Ahmad).

0272-8842/$ - see front matter © 2013 Elsevier Ltd and Techna Group S.r.l. All rights reserved.
http://dx.doi.org/10.1016/j.ceramint.2013.04.051

holes can be trapped by the oxygen and surface hydroxyl, respectively, to ultimately produce the hydroxyl radicals (•OH), which are known as the primary oxidizing species; and (3) the hydroxyl radicals commonly mineralize the adsorbed organic substances [9]. However, the photoexcited electrons and holes can also recombine to reduce photocatalytic efficiency of the semiconductor material [10]. Therefore, suppression of the recombination of photogenerated electron–hole pairs in the semiconductors is essential for improving their photocatalytic efficiency [11,12]. Doping of transition metals, noble metals and non-metals is a very expedient way to improve the electron–hole separation in semiconductor systems; many dopants such as La, Al, Sm, Ag and N have been used [9,13–17] and showed better photocatalytic performance.

It is also accepted that the surface area and surface defects play an important role in photocatalytic activities of metal oxide semiconductors, which could be accredited to the variation of the surface area, surface defects and band gap energy caused by the incorporation of dopant ions. It has been reported that the surface conditions of ZnO can be modified with the incorporation of dopant ions to enhance its photocatalytic activity [13–16]. Doping is an effective and facile method to modify the physical properties of the base materials and this will also expand the applications of base materials [1]. It has also been demonstrated that the structural and morphological characters such as particle size, shape, crystallinity, photocatalytic activity and some relevant properties of ZnO can be significantly affected by the method used during its synthesis [18]. Various approaches have been developed to prepare ZnO photocatalyst with special performance, which mainly include template method, solution combustion, precipitation, gas-phase reaction, hydrothermal synthesis and microwave heating [19–21].

In this study 0, 1, 2, 3, 4 and 6 mol% hafnium doped ZnO photocatalysts were synthesized by the sol–gel method. The microstructure, morphology and optical properties of the photocatalyst changes by hafnium doping were characterized by X-ray diffraction (XRD), X-ray photoelectron spectroscopy (XPS), scanning electron microscopy (SEM), transmission electron microscopy (TEM), photoluminescence (PL) emission spectra, FT-IR and UV–vis diffuse reflectance spectra (DRS). The photocatalytic activity of all the prepared photocatalysts under sunlight illumination was evaluated by the degradation of MB.

2. Experimental

2.1. Synthesis of ZnO and Hf-doped ZnO nanoparticles

All reagents were of analytical grade and were used without further purification. The materials selected for this experimental work were zinc acetate [$Zn(CH_3COOH)_2 \cdot 2H_2O$], hafnium oxide [$HfO_2$], nitric acid [$HNO_3$] and ethanol [$C_2H_5OH$]· having 99.0% purity, supplied by Merck. Undoped ZnO and Hf-doped ZnO were synthesized using a simple sol–gel method. The undoped ZnO was prepared by using zinc acetate and ethanol. For preparing Hf-doped ZnO, 1, 2, 3, 4, or 6 mol % of HfO_2 were countered with appropriate amount of nitric acid to create hafnium nitrate then zinc acetate and hafnium nitrate were taken in a round bottom flask. This was followed by gradual addition of ethanol to the solution under vigorous magnetic stirring. The resultant mixture was further stirred for 3 h at 80 °C and then kept at room temperature in air for 12 h to form an aged homogeneous gel. Subsequently, the as-prepared gel was dried at 100 °C in an oven; gel was porphyrized into powders and calcined at 500 °C in a furnace for 3 h. The ZnO doped with 1, 2, 3, 4 and 6 mol% of hafnium were labeled as samples 1 mol% Hf-ZnO, 2 mol% Hf-ZnO, 3 mol% Hf-ZnO, 4 mol% Hf-ZnO and 6 mol% Hf-ZnO, respectively.

2.2. Characterization

The XRD patterns were recorded using the Cu Kα radiation (λ=1.5406 Å) of a Shimadzu XD-5A diffractometer. Typical 2θ spectra were collected between 15° and 75°. Diffuse reflectance spectra were recorded on Hitachi U-4100 UV–vis spectrophotometer in the wavelength range of 300–600 nm. The nanopowders were pressed into pellets and $BaSO_4$ was used as a reference standard for correction of the instrumental background. The reflectance was converted to absorbance by the Kubelka–Munk function: $F(R) \propto K/S = (1-R)^2/2R$, where K is the absorption coefficient, S is the scattering coefficient, and R is the diffuse reflectance. The photoluminescence (PL) emission spectra were recorded using a HITACHI F-4500 Fluorescence spectrophotometer. The sample excitation was done at 325 nm at room temperature and the PL emission spectra were collected in the range of 375–600 nm using Xe lamp as radiation source. These powders were also characterized by using scanning electron microscope (SEM, HITACHI S-4800) and transmission electron microscope (TEM, JEOL JEM-1200EX). For IR measurements in the range 4000–400 cm^{-1}, a Nicolet Avatar 360 FTIR was used. X-ray photoelectron spectroscopy (XPS, Thermo-VG Scientific, ESCALAB 250, a monochromatic Al Kα X-ray source) was used for elemental and chemical compositional analysis of the samples.

2.3. Photocatalytic activity measurement

The photocatalytic activity of pure ZnO and Hf-doped ZnO photocatalysts were studied by using MB degradation. Experiments were performed under sunlight illumination in July 2011 in Multan (Pakistan) and the light intensity was measured with an irradiatometer (FZ-A, Photoelectric Instrument Factory, Beijing). The whole set-up was positioned in sunlight between 10am and 2pm. and the average intensity of sunlight during this period is about 1.263×10^5 lx unit. Experimental conditions are as follows: initial MB aqueous solution was 0.25 g/L; catalyst concentration was 25 mg/100 ml, taken in beaker covered with thin plastic sheet to avoid evaporation of the dye solution under sunlight. The suspension was magnetically stirred for 30 min to reach the adsorption/desorption equilibrium without sunlight exposure. Following this, the photocatalytic reaction was started by the exposure

of sunlight. The temperature of the suspension was kept at about 20 °C by an external cooling jacket with recycled water. After a setup exposure time, 5 ml suspension was sampled, centrifuged, and the supernatant was taken out for UV–vis absorption measurement. The intensity of the main absorption peak (660 nm) of the MB dye was referred to as the measure of the residual MB concentration.

3. Results and discussion

X-ray diffraction patterns of undoped ZnO and Hf-doped ZnO photocatalysts with different hafnium doping concentrations are shown in Fig. 1. The patterns clearly showed peaks of wurtzite structure of ZnO, namely, the planes (100), (002), (101), (102), (110), (103), (112), and (201) at 2θ values of ca. 32.03°, 34.68°, 36.49°, 47.77°, 56.76°, 63.05°, 68.11° and 69.34° respectively, which all are in good agreement with JCPDS File no. 05-0664 and literature findings [22,23]. Moreover, all Hf doped samples showed no extra peaks due to hafnium, zinc hafnium or any other oxide phase, indicating that the as-synthesized samples are of single phase [24]. A slight shift of peaks toward lower 2θ values was noted after Hf doping in all XRD patterns. The lattice parameters of Hf-doped ZnO were calculated, and were found to be slightly larger than those of undoped ZnO. This increase in lattice parameters might be attributed to the larger ionic radius of Hf^{4+} (0.78 Å) compared to that of Zn^{2+} (0.74 Å) [24]. The length of both lattice parameters "*a*,*c*" was increased with increasing Hf doping. The expansion of the lattice constants and the slight shift of XRD peaks with Hf doping confirmed that the hafnium was doped into the ZnO structure [22]. The average crystallite size (d) estimated from full-width at half-maxima of the (101) peak of the wurtzite ZnO by using the Scherrer formula ($d = k\lambda/\beta \cos\theta$) showed an approximate value of 17 to 14 nm (Table 1). The crystallite size of the ZnO nanopowders was decreased for doping content of 2 mol% and then increased for the doping of 3, 4, and 6 mol%.

Particle size and morphology of the selective photocatalysts were investigated using SEM and TEM (Fig. 2). SEM images showed surface and grain morphology of ZnO powders while TEM images showed the size of particles and the manner of particle distribution in the samples. The TEM images clearly showed that the particles were homogeneous and their size was approximately the same as that calculated by the Scherrer formula. The values of lattice parameters (a), (c) and (c/a) were calculated for undoped ZnO and Hf-doped ZnO photocatalysts, which were very close to result of wurtzite phase as reported previously [22,25]. Density plays a significant role in analyzing physical properties of samples. The X-ray or theoretical density D_x of the samples can be measured by using the following equation: $D_x = ZM/N_A V$. Where $Z=2$ (number of molecules per unit cell) [26], M is molecular weight, N_A is Avogadro's number (6.023×10^{23} mol^{-1}) and V is the volume of unit cell ($\sqrt{3}/2\ a^2 c$). The changes in X-ray density as a function of hafnium content is shown in Table 2. The decreasing trend in X-ray density was due to the increase in volume of hexagonal unit cell of ZnO.

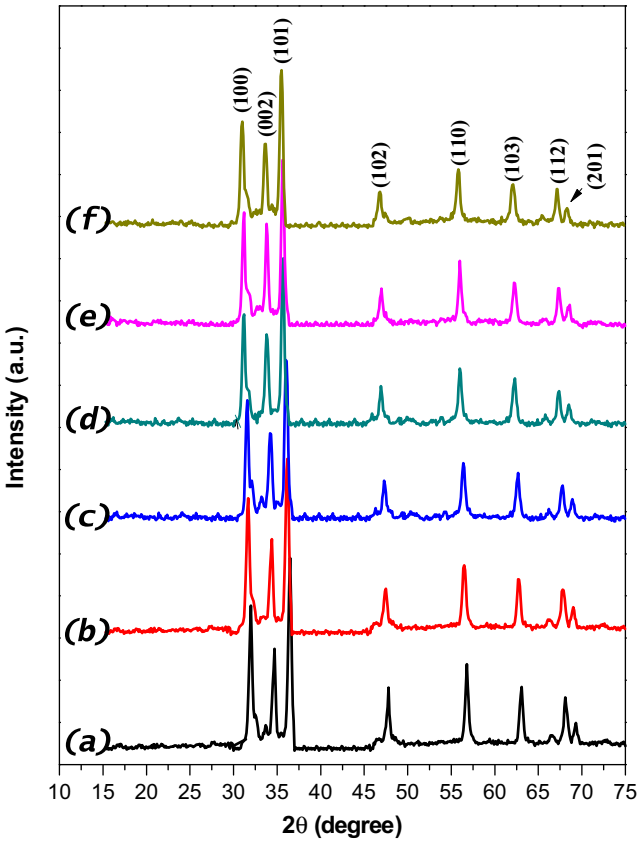

Fig. 1. XRD patterns of (a) ZnO (b) 1 mol% Hf-ZnO (c) 2 mol% Hf-ZnO (d) 3 mol% Hf-ZnO (e) 4 mol% Hf-ZnO and (f) 6 mol% Hf-ZnO.

Table 1
Values of crystallite size, and lattice parameters "a", "c", "c/a" ratio for ZnO, 1 mol% Hf-ZnO, 2 mol% Hf-ZnO, 3 mol% Hf-ZnO, 4 mol% Hf-ZnO and 6 mol% Hf-ZnO photocatalysts.

Samples	Crystallite size (nm)	Lattice parameter "a" [Å]	Lattice parameter "c" [Å]	Ratio "c/a"
ZnO	17	3.22	5.18	1.60
1 mol% Hf-ZnO	15	3.23	5.23	1.62
2 mol% Hf-ZnO	14	3.24	5.26	1.62
3 mol% Hf-ZnO	15	3.25	5.27	1.62
4 mol% Hf-ZnO	15	3.25	5.28	1.62
6 mol% Hf-ZnO	16	3.27	5.29	1.62

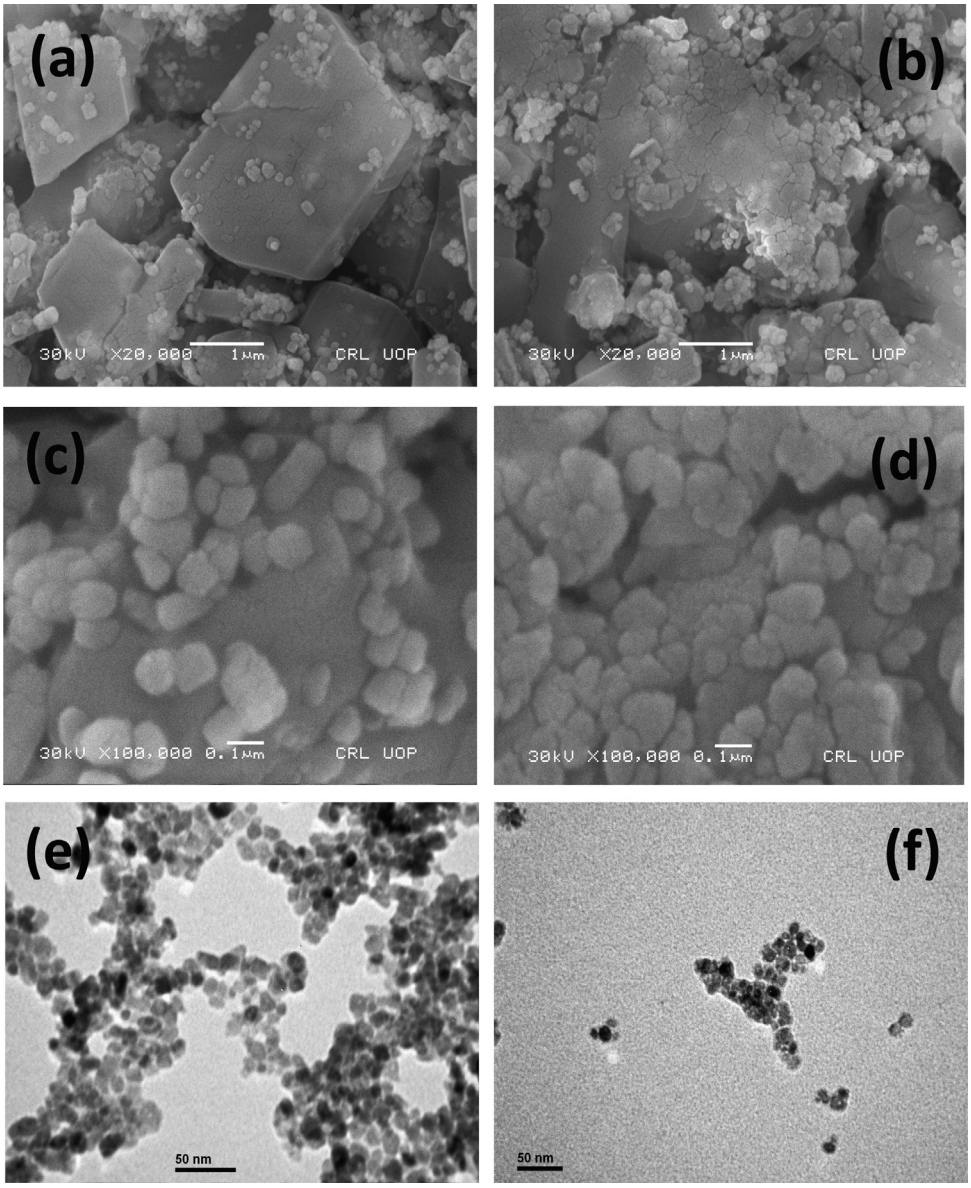

Fig. 2. SEM images of (a) ZnO (b) 2 mol% Hf-ZnO at lower magnification (c) ZnO (d) 2 mol% Hf-ZnO at higher magnification and TEM images of (c) ZnO and (d) 2 mol% Hf-ZnO photocatalysts.

Table 2
X-ray density, volume and band gap of ZnO, 1 mol% Hf-ZnO, 2 mol% Hf-ZnO, 3 mol% Hf-ZnO, 4 mol% Hf-ZnO and 6 mol% Hf-ZnO photocatalysts.

Samples	X-ray density "D_x" [g/cm^3]	Volume [(Å)^3]	Band gap (eV)
ZnO	5.82	46.51	3.26
1 mol% Hf-ZnO	5.68	47.25	3.24
2 mol% Hf-ZnO	5.64	47.22	3.23
3 mol% Hf-ZnO	5.62	48.29	3.21
4 mol% Hf-ZnO	5.60	48.30	3.19
6 mol% Hf-ZnO	5.57	48.98	3.17

For the FT-IR analysis, KBr pellets were prepared for pure and hafnium doped ZnO photocatalysts. The IR measurements were carried out in the range of 4000–400 cm^{-1} in order to verify the preparation of nanocrystalline ZnO photocatalyst and to identify the adsorbed impurities at the surface of ZnO photocatalyst. Fig. 3 exhibited the FTIR spectra of undoped ZnO and 2 mol% Hf-ZnO samples. In IR spectra of undoped ZnO and 2 mol% Hf-ZnO samples, the strong peaks at 3450,

1642 cm^{-1} originated from surface adsorbed water and hydroxyl groups. The weak absorption bands located at ~2920, 2350, 1429 and 1051 cm^{-1} were related to C–H mode, atmospheric CO_2, OH bending vibration of C–OH and C–O stretching vibration respectively. In both IR spectra, the significant absorption band in the region 430–450 cm^{-1} was assigned to the characteristic absorption band of ZnO.

X-ray photoelectron spectroscopy (XPS) measurements were carried out to determine the chemical states of elements in the 2 mol% Hf-ZnO photocatalyst. The survey spectrum (Fig. 4) indicated that the sample was composed of Zn, O and Hf, and no peaks of other elements were observed. The two peaks detected at the energy positions of 1010–1050 eV correspond to the Zn 2p3/2 and Zn 2p1/2 orbitals. The high-resolution scan of

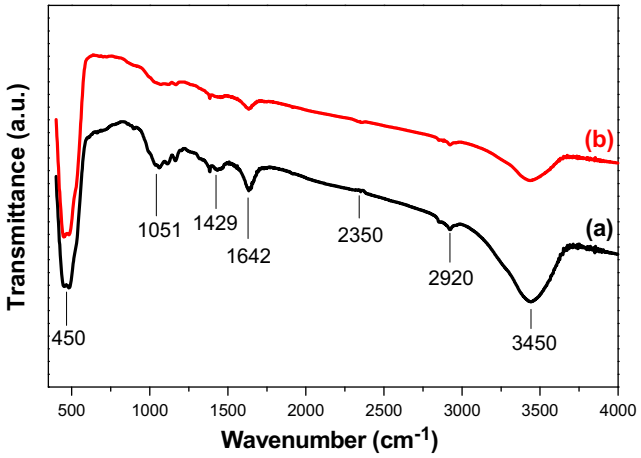

Fig. 3. FTIR spectra of (a) ZnO and and (b) 2 mol% Hf-ZnO photocatalysts.

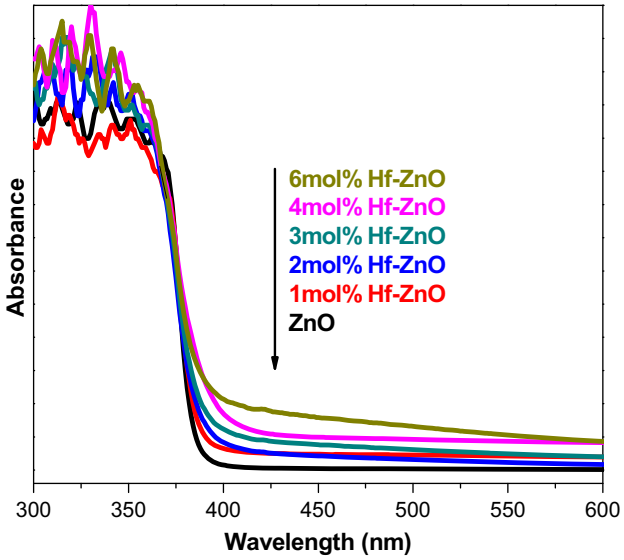

Fig. 5. UV–vis absorption spectra of ZnO and Hf-doped ZnO photocatalysts.

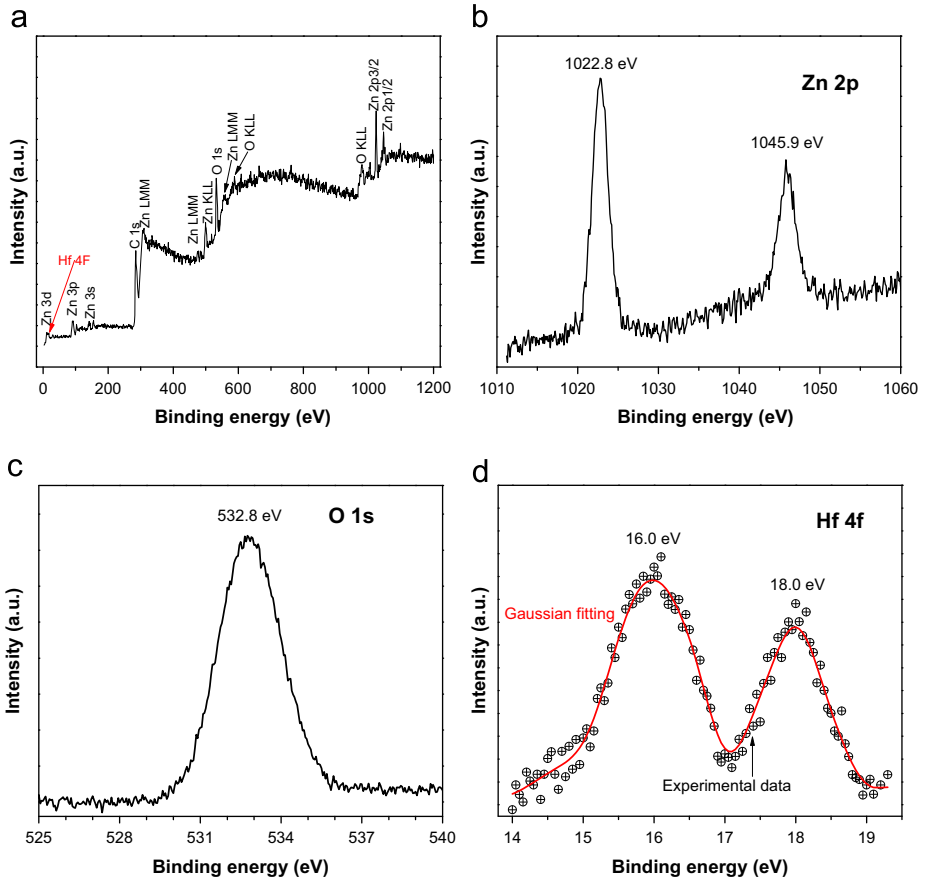

Fig. 4. XPS survey spectra and high resolution spectra of Zn 2p, O 1s and Hf 4f region for 2 mol% Hf-ZnO photocatalyst.

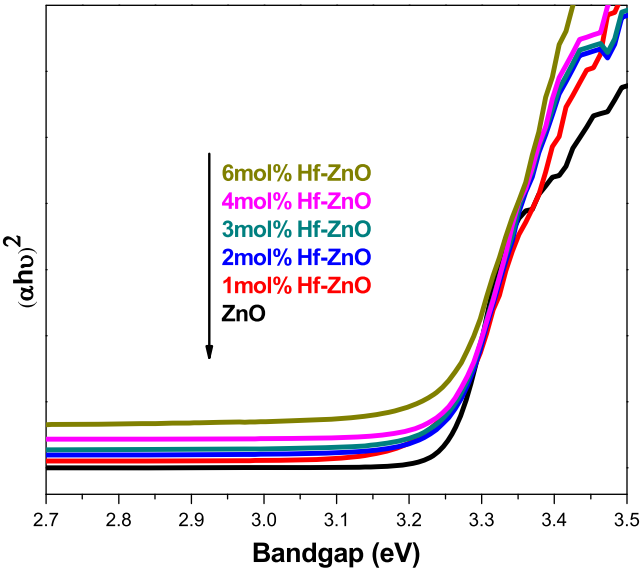

Fig. 6. Plots of $(\alpha h\upsilon)^2$ versus photon energy ($h\upsilon$) of ZnO and Hf-doped ZnO photocatalysts.

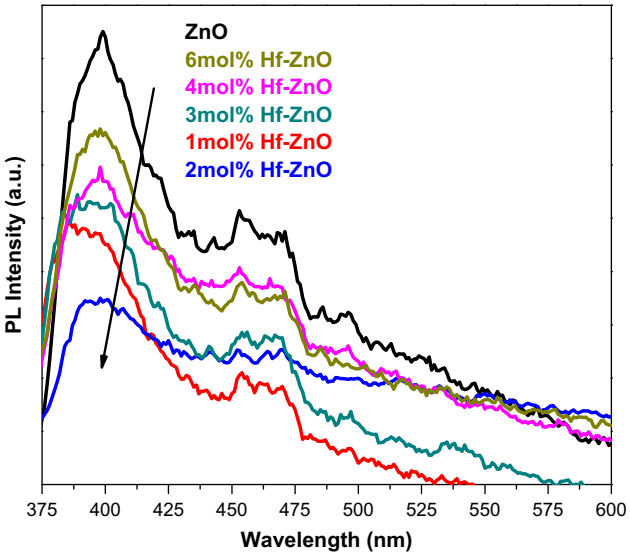

Fig. 7. Photoluminescence spectra of ZnO and Hf-doped ZnO photocatalysts.

Zn 2p showed the exact peak location of Zn 2p3/2 at 1022.8 eV and of Zn 2p1/2 at 1045.9 eV [27]. In O 1s core level spectrum, the single peak observed at 532.8 eV can be attributed to chemisorbed oxygen caused by the surface hydroxyl [9]. Finally, in Hf 4f core level spectrum, two peaks at binding energies 16.0 eV and 18.0 eV confirmed the presence of Hf in the doped sample [28].

UV–vis spectroscopy study was conducted on all the photocatalysts to observe the changes in optical properties as a function of material composition. The UV–vis diffuse absorption spectra of undoped and doped ZnO photocatalysts with different hafnium contents are shown in Fig. 5. The band edge for the undoped ZnO sample appeared at 378 nm while the band edges of the Hf-doped ZnO samples were shifted toward longer wavelength regions along with stronger absorption intensities for the higher hafnium concentration samples. Typically, the light absorption edge extended to 388, 391, 396, 401 and 408 nm as hafnium was incorporated into ZnO matrix with 1, 2, 3, 4 and 6 mol% respectively. The absorbance coefficient (α) was calculated from the raw absorbance data to obtain the optical band gap (E_g). The band gap values were thus determined by the extrapolation of the linear portion of the $(\alpha h\upsilon)^2$ curve versus the photon energy $h\upsilon$ (Table 2). With increasing the hafnium content from 0.0 to 6.0 mol%, the band gap energies decreased continuously from 3.26 to 3.17 eV (Fig. 6). The slight decrease of band gap was possibly due to the doping which might have caused band edge bending [29]. The red shift of the band gap edge with incorporation of Hf into ZnO has also been reported [30] and interpreted to be due to the sp–d exchange interactions between the band electrons and the localized d electrons of the Hf^{4+} ions substituting Zn ions [31].

Fig. 7 shows the photoluminscence emission spectra of ZnO and Hf-doped ZnO photocatalysts. Photoluminescence spectra exhibited five main emission peaks at about 399, 422, 443, 453 and 469 nm with excitation at 325 nm. A broad peak around 399 nm is attributed to the near band-edge emission of ZnO. Other peaks observed at 422 nm can be ascribed to divalent zinc vacancy and 469 nm to intrinsic defects such as interstitial zinc and oxygen [32,33]. The small peak observed at 443 nm corresponds to the transition of electrons from shallow donor levels of oxygen vacancies to the valence band and the peak at 463 nm is assigned to electronic transition from shallow donor levels of zinc interstitial to the valence band [34]. All these peaks were observed for undoped as well as for Hf-doped ZnO. It is seen that the positions of the peaks are similar, while their intensities are quite different. It is known that the PL emission is a result of the recombination of excited electrons and holes, the lower PL intensity may indicate the lower recombination rate of electrons and holes under light irradiation. It is renowned that the photoluminescence of ZnO is sensitive to the defects in the material [35,36]. The PL intensity of ZnO was highest among all the samples, demonstrating the higher recombination of electrons and holes. The emission intensities were significantly weakened with hafnium doping, which implies that the recombination of charge carriers was effectively suppressed. Among all the samples the lowest intensity was observed for the 2 mol% Hf-ZnO sample, suggesting that the charge carriers were separated more effectively due to the effect of hafnium doping. However, 3, 4 and 6 mol% Hf-ZnO exhibited significant increases in PL emission intensities compared to that of 2 mol % Hf-ZnO. This may be due to the fact that the excess introduction of Hf^{4+} in to ZnO lattice also acts as the recombination center, which is detrimental to the photocatalytic activity.

The photocatalytic degradation of highly concentrated MB aqueous solution (250 mg/l) using very small amount of pure and doped ZnO photocatalysts (25 mg/100 ml) under sunlight irradiation are shown in Fig. 8. Phototcatalytic degradation of MB follows roughly the pseudo-first-order reaction kinetics for low dye concentrations [37]:

$$ln(C_o/C) = k_{app}t$$

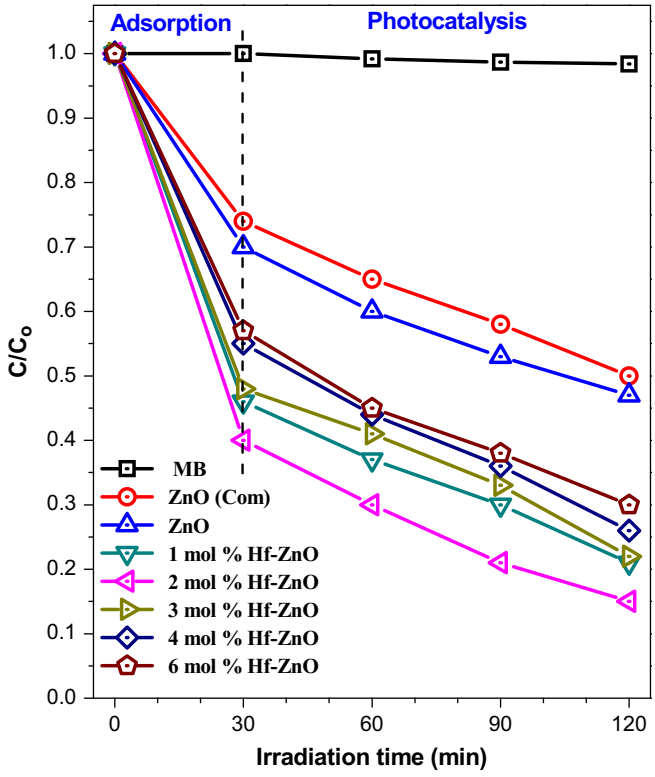

Fig. 8. Time profiles of C/C_o for various photocatalysts under sunlight irradiation.

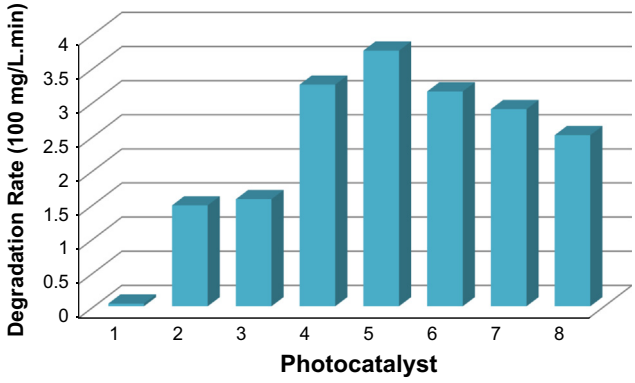

Fig. 9. The initial degradation rate r_o (mg l^{-1} min^{-1}) of photocatalysts in methylene blue aqueous solution; (1) MB (2) ZnO commercial (3) ZnO (4) 1 mol% Hf-ZnO (5) 2 mol% Hf-ZnO, (6) 3 mol% Hf-ZnO (7) 4 mol% Hf-ZnO and (8) 6 mol% Hf-ZnO photocatalysts under sunlight irradiation.

where k_{app} is the apparent constant, used as the basic kinetic parameter for different photocatalysts. C_o is the initial concentration of MB in aqueous solution and C is the residual concentration of MB at time t. The apparent constant values could be deduced from the linear fitting of $ln(C_o/C)$ versus irradiation time. The initial degradation rate ($r_o = k_{app}C_o$) of 250 mg l^{-1} MB with different photocatalysts was studied and the results are presented in Fig. 9. The results showed that degradation rate (r_o) was enhanced by hafnium doping. The degradation rate constant for 2 mol% Hf-ZnO catalyst ($r_o = 3.75$ min^{-1}) was found to be higher than that of undoped ZnO ($r_o = 1.53$ min^{-1}) and commercial ZnO ($r_o = 1.47$ min^{-1}). It was found that pure ZnO had little ability to degrade MB under sunlight irradiation and all the Hf-doped ZnO photocatalysts exhibited higher photocatalytic activity than that of pure ZnO under sunlight. The order of photocatalytic activity of Hf-doped ZnO after 120 min was as follows: 2 mol% Hf-ZnO > 1 mol% Hf-ZnO > 3 mol% Hf-ZnO > 4 mol% Hf-ZnO > 6 mol% Hf-ZnO > ZnO > ZnO commercial, which advocated that Hf doping has enhanced the photocatalytic activity of ZnO. 2 mol% Hf-doped ZnO photocatalyst showed the highest photocatalytic degradation efficiency; with the MB concentration reduction by 85% in 120 min (Fig. 8). Firstly, the enhanced photocatalytic activity of hafnium doped ZnO catalyst might be attributed to extended light absorption in the visible-light region due to Hf doping. Secondly, the presence of Hf into ZnO favors the transfer of photogenerated electrons to Hf and then Hf acts as a reservoir for these electrons, thereby promoting an interfacial charge-transfer process and hence the rate of degradation of MB was significantly increased. This can be attributed to suppressed recombination of photogenerated electron–hole pairs due to presence of hafnium in the ZnO photocatalyst.

4. Conclusions

Pure ZnO and Hafnium doped ZnO photocatalysts were synthesized using a facile sol–gel method. It was found that all the doped samples had stronger light absorption in visible light range when compared with the pure ZnO. The doped ZnO photocatalysts showed enhanced photocatalytic activity than pure ZnO under sunlight irradiation for MB degradation. The 2 mol% Hf-doped ZnO photocatalyst demonstrated the highest photocatalytic degradation efficiency which was about 85% in 120 min. All these results indicated that doped ZnO is a potential candidate for the practical application in photocatalytic degradation of organic contaminant.

Acknowledgements

The author M. Ahmad thanks the Higher Education Commission of Pakistan for financial support and also gratefully acknowledged the support of State Key Laboratory of Silicon Materials, Department of Materials Science and Engineering, Zhejiang University, China.

References

[1] J.C. Sin, S.M. Lam, K.T. Lee, A.R. Mohamed, Preparation and photocatalytic properties of visible light-driven samarium-doped ZnO nanorods, Ceramics International, 39 (2013) 5833–5843.

[2] K.C. Hsiao, S.C. Liao, Y.J. Chin, Synthesis, characterization and photocatalytic property of nanostructured Al-doped ZnO powders prepared by spray pyrolysis, Materials Science and Engineering A 447 (2007) 71–76.

[3] V.R. Shinde, T.P. Gujar, C.D. Lokhande, R.S. Mane, S.H. Han, Mn doped and undoped ZnO films: a comparative structural, optical and

electrical properties study, Materials Chemistry and Physics 96 (2006) 326–330.
[4] J.H. Sun, S.Y. Dong, J.L. Feng, X.J. Yin, X.C. Zhao, Enhanced sunlight photocatalytic performance of Sn-doped ZnO for methylene blue degradation, Journal of Molecular Catalysis A: Chemical 335 (2011) 145–150.
[5] A. McLaren, T.V. Solis, G. Li, S.C. Tsang, Shape and size effects of ZnO nanocrystals on photocatalytic activity, Journal of the American Chemical Society 131 (2009) 12540–12541.
[6] Y.J. Kwon, K.H. Kim, C.S. Lim, K.B. Shim, Characterization of ZnO nanopowders synthesized by the polymerized complex method via an organochemical route, Journal of Ceramic Processing Research 3 (2002) 146–149.
[7] S.F. Chen, W. Zhao, W. Liu, S.J. Zhang, Preparation, characterization and activity evaluation of p–n junction photocatalyst p-ZnO/n-TiO_2, Applied Surface Science 255 (2008) 2478–2484.
[8] S. Rehman, R. Ullah, A.M. Butt, N.D. Gohar, Strategies of making TiO_2 and ZnO visible light active, Journal of Hazardous Materials 170 (2009) 560–569.
[9] C. Ren, B. Yang, M. Wu, J. Xu, Z. Fu, Y. Lv, T. Guo, Y. Zhao, C. Zhu, Synthesis of Ag/ZnO nanorods array with enhanced photocatalytic performance, Journal of Hazardous Materials 182 (2010) 123–129.
[10] L.R. Zheng, Y.H. Zheng, C.Q. Chen, Y.Y. Zhan, X.Y. Lin, Q. Zheng, K. M. Wei, J.F. Zhu, Network structured SnO_2/ZnO heterojunction nanocatalyst with high photocatalytic activity, Inorganic Chemistry Communications 48 (2009) 1819–1825.
[11] C. Wang, X.M. Wang, B.Q. Xu, J.C. Zhao, B.X. Mai, P.A. Peng, G. Y. Sheng, J.M. Fu, Enhanced photocatalytic performance of nanosized coupled ZnO/SnO_2 photocatalysts for methyl orange degradation, Journal of Photochemistry and Photobiology A: Chemistry 168 (2004) 47–52.
[12] N.R. Khalid, E. Ahmed, Z.L. Hong, Y.W. Zhang, M. Ullah, M. Ahmad, Graphene modified Nd/TiO_2 photocatalysts for methyl orange degradation under visible light irradiation, Ceramics International, 39 (2013) 3569–3575.
[13] S. Suwanboon, P. Amornpitoksuk, A. Sukolrat, N. Muensit, Optical and photocatalytic properties of La-doped ZnO nanoparticles prepared via precipitation and mechanical milling method, Ceramics International 39 (2013) 2811–2819.
[14] M. Ahmad, E. Ahmed, Y.W. Zhang, N.R. Khalid, J.F. Xu, M. Ullah, Z. L. Hong, Preparation of highly efficient Al-doped ZnO photocatalyst by combustion synthesis, Current Applied Physics 13 (2013) 697–704.
[15] F. Meng, J. Li, Z.L. Hong, M. Zhi, A. Sakla, C. Xiang, N.Q. Wu, Photocatalytic generation of hydrogen with visible-light nitrogen-doped lanthanum titanium oxides, Catalysis Today 199 (2013) 48–52.
[16] F. Meng, Z.L. Hong, J. Arndt, M. Li, M. Zhi, F. Yang, N.Q. Wu, Visible light photocatalytic activity of nitrogen-doped $La_2Ti_2O_7$ nanosheets originating from band gap narrowing, Nano Research 5 (2012) 213–221.
[17] J. Wang, D.N. Tafen, J.P. Lewis, Z.L. Hong, A. Manivannan, M. Zhi, M. Li, N.Q. Wu, Origin of photocatalytic activity of nitrogen-doped TiO_2 nanobelts, Journal of the American Chemical Society 131 (2009) 12290–12297.
[18] W.D. Yu, X.M. Li, X.D. Gao, F. Wu, Large-scale synthesis and microstructure of SnO_2 nanowires coated with quantum-sized ZnO nanocrystals on a mesh substrate, Journal of Physical Chemistry B 109 (2005) 17078–17081.
[19] Y. Zhang, W.F. Zhang, H.W. Zheng, Fabrication and photoluminescence properties of ZnO: Zn hollow microspheres, Scripta Materialia 57 (2007) 313–316.
[20] T.H. Lea, Q.D. Truong, T. Kimura, H. Li, C. Guo, S. Yin, T. Sato, Y. C. Ling, Synthesis of hierarchical porous ZnO microspheres and its photocatalytic deNO_x activity, Ceramics International 38 (2012) 5053–5059.
[21] S.M. Wang, Z.S. Yang, M.K. Lu, Y.Y. Zhou, G.J. Zhou, Z.F. Qiu, S. F. Wang, H.P. Zhang, A.Y. Zhang, Co-precipitation synthesis of hollow Zn_2SnO_4 spheres, Materials Letters 61 (2007) 3005–3008.
[22] Joint Committee on Powder Diffraction Standards (JCPDS), File no. 05-0664.
[23] M. Ahmad, Z.L. Hong, E. Ahmed, N.R. Khalid, A. Elhissi, W. Ahmad, Effect of fuel to oxidant molar ratio on the photocatalytic activity of ZnO nanopowders, Ceramics International 39 (2013) 3007–3015.
[24] S. Senthilkumaar, K. Rajendran, S. Banerjee, T.K. Chini, V. Sengodan, Influence of Mn doping on the microstructure and optical property of ZnO, Materials Science in Semiconductor Processing 11 (2008) 6–12.
[25] C.C. Hwang, T.Y. Wu, Synthesis and characterization of nanocrystalline ZnO powders by a novel combustion synthesis method, Materials Science and Engineering B 111 (2004) 197–206.
[26] S. Desgreniers, High-density phases of ZnO: structural and compressive parameters, Physical Review B 58 (1998) 14102–14105.
[27] L. Ai, C. Zhang, Z. Chen, Removal of methylene blue from aqueous solution by a solvothermal synthesized graphene/magnetite composite, Journal of Hazardous Materials 192 (2011) 1515–1524.
[28] J.F. Moulder, W.F. Stickle, P.E. Sobol, K.D. Bomben, Handbook of X-ray Photoelectron Spectroscopy, Perkin-Elmer Corporation, Minnesota, 1992.
[29] S.Y. Bae, C.W. Na, J.H. Kang, J. Park, Comparative structure and optical properties of Ga-, In-, and Sn-doped ZnO nanowires synthesized via thermal evaporation, Journal of Physical Chemistry B 109 (2005) 2526–2531.
[30] Q. Xiao, J. Zhang, C. Xiao, X. Tan, Photocatalytic decolorization of methylene blue over $Zn_{1-x}Co_xO$ under visible light irradiation, Journal of Materials Science and Engineering 142 (2007) 121–125.
[31] Y.D. Kim, S.L. Cooper, M.V. Klein, B.T. Jonker, Spectroscopic ellipsometry study of the diluted magnetic semiconductor system Zn (Mn,Fe,Co)Se, Physical Review B 49 (1994) 1732–1742.
[32] M.V. Limaye, S.B. Singh, R. Das, P. Poddar, S.K. Kulkarni, Room temperature ferromagnetism in undoped and Fe doped ZnO nanorods: microwave-assisted synthesis, Journal of Solid State Chemistry 184 (2011) 391–400.
[33] A.K. Singh, V. Viswanath, V.C. Janu, Synthesis, effect of capping agents, structural, optical and photoluminescence properties of ZnO nanoparticles, Journal of Luminescence 129 (2009) 875–878.
[34] E. De la Rosa, S. Sepulveda-Guzman, B. Reeja-Jayan, A. Torres, P. Salas, N. Elizondo, M. Jose Yacaman, Controlling the growth and luminescence properties of well-faceted ZnO nanorods, Journal of Physical Chemistry C 111 (2007) 8489–8495.
[35] P. Sagar, P.K. Shishodia, R.M. Mehra, H. Okada, A. Wakahara, A. Yoshida, Photoluminescence and absorption in sol–gel-derived ZnO films, Journal of Luminescence 126 (2007) 800–806.
[36] S. Fujihara, Y. Ogawa, A. Kasai, Tunable visible photoluminescence from ZnO thin films through Mg-doping and annealing, Chemistry of Materials 16 (2004) 2965–2968.
[37] N.R. Khalid, Z.L. Hong, E. Ahmed, Y.W. Zhang, H. Chan, M. Ahmad, Synergistic effects of Fe and graphene on photocatalytic activity enhancement of TiO_2 under visible light, Applied Surface Science 258 (2012) 5827–5834.